

# DEFECT SUBSTRUCTURES IN PLATE IMPACTED AND LASER SHOCKED MONOCRYSTALLINE COPPER

Bu Yang Cao<sup>1</sup>, Marc A. Meyers<sup>1</sup>, David H. Lassila<sup>2</sup>, Matt S. Schneider<sup>1</sup>, Yong Bo Xu<sup>3</sup>, Daniel H. Kalantar<sup>2</sup>, Bruce A. Remington<sup>2</sup>

<sup>1</sup>*MATS, Univ. of California, San Diego, 9500 Gilman Dr. La Jolla, CA 92093-0411 USA*

<sup>2</sup>*Lawrence Livermore National Laboratory, Livermore, CA 94550 USA*

<sup>3</sup>*Chinese Academy of Sciences, Inst. of Metal, Shenyang, Liao Ning 110016 China*

**Abstract.** Monocrystalline copper samples with orientations of [001] and [221] were shocked at pressures ranging from 20 GPa to 60 GPa using two techniques: direct drive lasers and explosively driven flyer plates. The pulse duration for these techniques differed substantially: 40 ns for the laser experiments at 0.5 mm into the sample and 1.1 ~1.4  $\mu$ s for the flyer-plate experiments at 5 mm into the sample. The residual microstructures were dependent on orientation, pressure, and shocking method. For the flyer-plate experiments, the longer pulse duration allow shock-generated defects to reorganize into lower energy configurations. Calculations show that the post shock cooling for laser shock is  $10^3 \sim 10^4$  faster than that of the plate-impact shock, propitiating recovery and recrystallization conditions for the latter. At the higher pressure level extensive recrystallization was observed in the plate-impact samples. An effect to contribute significantly to the recrystallization is the existence of micro-shearbands, which increase the local temperature.

**Keywords:** laser, shock compression, plate impact, shear localization in copper, shock waves, explosives

**PACS:** 62.50.+p

## INTRODUCTION

Flyer-plate impact and laser shock are two typical loading methods employed in shock-recovery experiments. Significant differences in the residual microstructure in monocrystalline copper shocked by these two methods have been observed. The objective of this paper is to demonstrate the differences of the residual microstructures are to a large extent due to how the heat generated inside the samples during shock is extracted. Post-shock recovery and recrystallization processes dominate the residual microstructures, if the time interval and temperature are sufficient. The unique advantage of laser shock compression

over plate impact, namely, the rapid post-shock cooling, is discussed.

## EXPERIMENTAL PROCEDURE

Explosively driven flyer plates and direct drive lasers produce different shock pulses. For the plate impact experiments reported herein, the duration of the pulse at a depth of 5 mm from the impact interface was in the 1.1—1.4  $\mu$ s range. The triangular shape laser shock pulse duration is 40 ns at energy around 300 J, which produces an initial pressure of approximately 60 GPa. The facilities used for plate impact and laser shock have been described in previous papers [1,2]. Monocrystalline coppers with orientations of  $\langle 001 \rangle$  and  $\langle 221 \rangle$  were shock-compressed by both laser (at ambient

temperature) and plate impact (at 88 K) from 20 GPa to 60 GPa.

### EXPERIMENTAL RESULTS

The microstructures are characterized by stacking faults for both the 30-40 GPa plate impacted and laser shocked  $\langle 100 \rangle$  samples. The average spacing between stacking faults is 230 and 450 nm for the laser shocked samples and 180 and 220 nm for the plate impacted sample (Fig. 1(a)). It shows the two sets of stacking faults as the traces of  $[\bar{2}20]$  and  $[220]$  orientations in the (001) plane. Four stacking fault variants *viz* the  $(11\bar{1})1/6[112]$ ,  $(111)1/6[\bar{1}\bar{1}2]$ ,  $(\bar{1}11)1/6[1\bar{1}2]$ , and  $(\bar{1}\bar{1}1)1/6[\bar{1}12]$  are observed in 40 GPa laser shocked samples. The stacking faults are similar to the ones observed by Murr [3]. It should also be noted that, in the 30 GPa plate impacted  $\langle 100 \rangle$  samples, we observed isolated recrystallization as well as localized deformation bands. These were absent for the laser shocked specimens.

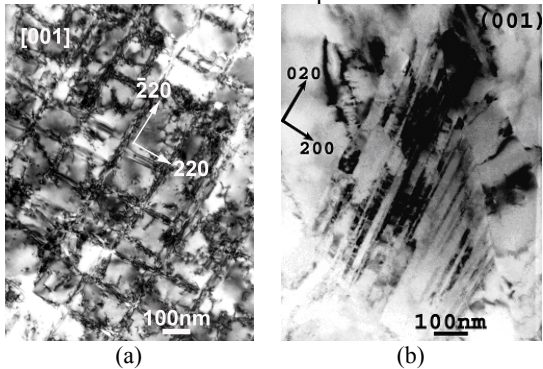


**Figure 1.** (a) Stacking faults in 30 GPa plate impacted  $\langle 100 \rangle$  sample; (b) Micro-bands in 30 GPa plate impacted  $\langle 221 \rangle$  samples.

The substructure of the plate impacted  $\langle 221 \rangle$  sample shocked at 30 GPa contains micro-bands, whose morphologies vary through this sample. Some large bands, shown in the left part of Fig. 1 (b), have a width around 120 ~130 nm. Micro-bands with a width of 20~30 nm were found within these large bands. Huang and Gray [4] proposed a model to explain the formation of micro-bands, based on the development of coarse slip bands. The laser shocked  $\langle 221 \rangle$  samples are characterized by a greater density of twins than bands. Although

some bands with width of 100 ~ 200 nm were observed very similar to those big bands in 30 GPa plate impacted samples, twins with  $(1\bar{1}1)$  habit plane were more prevalent throughout the sample.

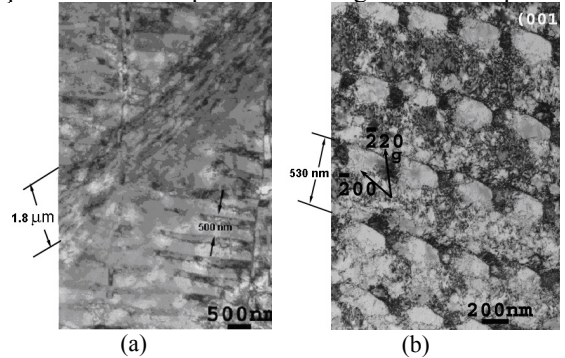


**Figure 2.** TEM for 57 GPa plate impacted  $\langle 100 \rangle$  copper samples: (a) overview of the sample (x10K); (b) dislocation circles.

At 55-60 GPa, Micro-twins occur in both plate impacted and laser shocked  $\langle 100 \rangle$  samples. There are micro-twins with  $(\bar{1}11)$  as habit plane in plate impacted samples. The sizes for micro-twins vary from 80 nm to 180 nm. For the laser-shocked samples, there are two sets of micro-twins along  $[220]$  and  $[\bar{2}20]$ .

For the 57 GPa plate impacted samples, there are deformation bands, slip bands, recrystallized regions and dislocation tangles in addition to micro-twins. Fig. 2 (a) shows a deformation band of approximately 1.8  $\mu\text{m}$  width traversing the specimen. The appearance of these stacking faults is different from the ones shown in Fig. 1(a). There is evidence for recovery processes within them. These broad bands are absent after laser shock because of the much smaller time. Indeed, the shock velocity is approximately 5.6 mm/ $\mu\text{s}$ . A duration of 1.4  $\mu\text{s}$  can generate heterogeneities extending over a few mm. On the other hand, laser shock, with duration of only 2ns, is much more restricted in its ability to generate inhomogeneities. In Fig. 2 (b), regular dislocation cell arrays can be seen. Between two arrays, there are dislocation tangles and in some places the density of dislocation is very high. Mughrabi and Ungár [5] found some dislocation cell structures very similar to our observations, but they are quite unlike the cells observed by other investigators (e.g., Johari and Thomas [6]). The distances between the

repeated structures in both Fig. 2 (a) and (b) have the same width of around 500 nm. The periodicity of the features of Fig. 2(a) is remarkable. It is speculated that these features are due to the recovered stacking-fault arrays seen in Fig. 2 (b). The major difference between the laser shocked samples and plate impacted samples in 55-60 GPa regime is the presence of fully recrystallized regions in the latter.

The <221> samples plate impacted at 57 GPa were full of large recrystallized grains (Fig. 3(a)). Annealing twins grow in the recrystallized grains. In 60 GPa laser shocked <221> samples, there is a high density of dislocation, as shown in Fig. 3(b). These dislocations are tangled and some bands were formed as a result of heavy dislocation density. A few of deformation twins were also found in this sample.

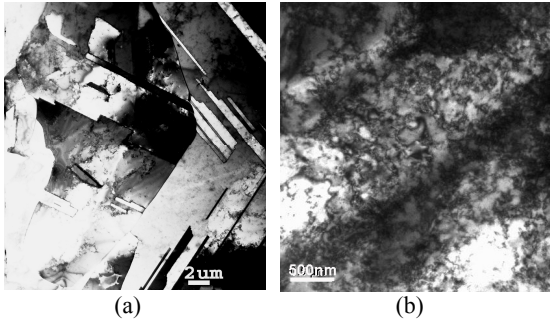


**Figure 3.** (a) TEM showing annealing twins and recrystallized grains in 57 GPa plate impacted <221> sample; (b) Dislocation structures in 60 GPa laser shocked <221> samples.

### ANALYSIS

It is important to notice that laser and plate-impact shocks have different wave shapes and duration times because this likely results in very different effects on the heat generated during the shock and the heat transfers afterwards. Based on the progress of the shock pulse and its decay, the residual temperatures immediately after shock can be calculated [7] (Fig. 4). To calculate the heat transfer after shock, a semi-infinite heat transfer model was adopted [8]. The following assumptions were made: 1) Conduction is one-dimensional; 2) Copper sample is a semi-infinite medium; 3)

Temperature profiles at time  $t=0$  are shown in Fig. 4.

Fig. 5 shows the change of temperature with time for 30 GPa plate impacted samples. The maximum temperature (at surface) changes from approximately 160 K to 100 K during a period of 1000 s. For 57 GPa (Fig.6), the temperature changes from 360 K to 140 K during this same time period. This period of time should be sufficient to induce some microstructural changes

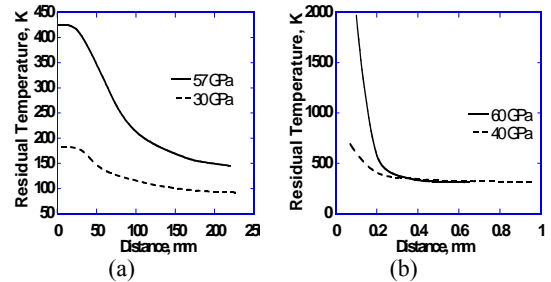


**Figure 4.** Residual temperature inside the sample immediately after shock: (a) plate-impact shock; (b) laser shock.

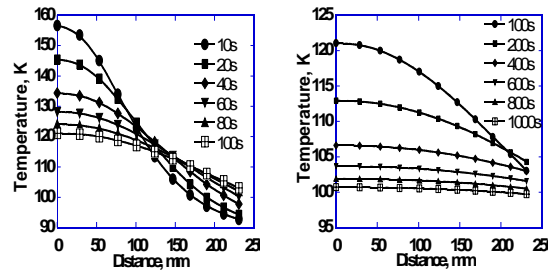


**Figure 5.** Temperature change for copper plate impacted at 30 GPa.

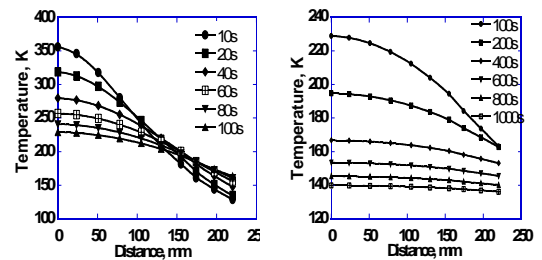


**Figure 6.** Temperature change for copper plate impacted at 57 GPa.

inside the samples. For laser shock, the region which is affected by the temperature rise is much shorter (up to 1mm). The temperature excursions in laser shocked samples are shown in Fig. 7. Based on these analyses, a qualitative comparison of the plate impact and laser shock can be estimated. The temperature decays in the laser shocked sample are  $10^3 \sim 10^4$  faster than those in the plate impacted sample. These results explain why, although the peak pressures of laser shock are much higher than those of impact (resulting in higher residual temperatures), the post-shock microstructures in plate impact samples show a greater effect of post shock thermal excursion.

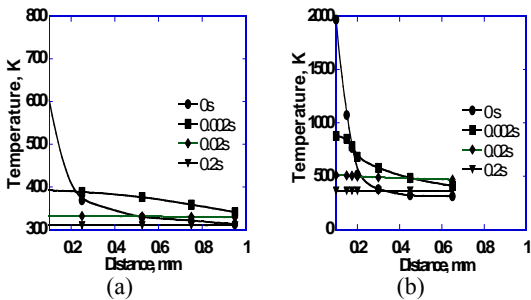


**Figure 7.** Temperature change in laser shocked copper: (a) at 200J (40 GPa); (b) at 300J (60 GPa).

TEM observations confirm the presence of localized regions of concentrated shear. The plastic deformation in these regions substantially exceeds those predicted from uniaxial strain, and one can expect local fluctuations in temperature. The temperature rise in the shear localization areas can be calculated as [1]:

$$\Delta T_d = \frac{\beta}{\rho C_p} \int_{\epsilon_0}^{\epsilon_1} \sigma d\epsilon \quad (1)$$

where  $C_p$  is the heat capacity, and  $\beta$  is the Taylor factor (0.9-1.0 here). We use the Johnson-Cook [9] equation strength of the material  $\sigma$ . The temperature change due to the plastic deformation is expressed as:

$$\frac{T - T_r}{T_m - T_r} = 1 - \exp\left[-\frac{0.9(1 + C \log \frac{\dot{\epsilon}}{\dot{\epsilon}_0})}{\rho C_p (T_m - T_r)} \times \left(\sigma_0 \epsilon + \frac{B \epsilon^{n+1}}{n+1}\right)\right] \quad (2)$$

Where,  $T_r = 90$  K,  $T_m = 1356$  K,  $B = 53.7$  MPa,  $C = 0.026$ ,  $\sigma_0 = 330$  MPa (the value for shock hardened copper),  $n = 0.56$ ,  $m = 1.04$ . There is considerable local heat generation around heavily deformed areas (such as deformation bands) as show in Fig. 8. These regions can act as initiation sites for post-shock recrystallization.

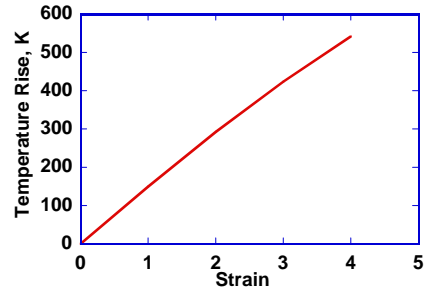


**Figure 8:** Temperature rise due to plastic deformation.

## ACKNOWLEDGEMENTS

Supported by DOE Grants DEFG0398DP00212 and DEFG0300SF2202.

## REFERENCES

1. D. H. Lassila, T. Shen, B. Y. Cao, and M. A. Meyers, *Metal. and Mat. Trans.*, 35A (2004) 2729-2739.
2. M. A. Meyers, F. Gregori, B. K. Kad, M. S. Shneider, D. H. Kalantar, B. A. Remington, G. Ravichandran, T. Boehly, J. S. Wark, *Acta Metall.* 51 (2003) 1211-1228.
3. L. E. Murr, in: M. A. Meyers and L. E. Murr (Eds.), *Shock Waves and High-Strain-Rate Phenomena in Metals*, Plenum, NY, 1981, pp. 607-673.
4. J. C. Huang and G. T. Gray III, *Acta metall.* 37. No. 12, (1989) 3335-3347.
5. H. Mughrabi, T. Ungár, W. Kienle, and M. Wilkens, *Phil. Mag. A*, 53 (1986) 793-813.
6. O. Johari and G. Thomas, *Acta Metall.* 12 (1964) 1153-1159.
7. M. A. Meyers, *Dynamic Behavior of Materials*, John Wiley and Sons, Inc, New York, 1994.
8. F. Kreith and M. S. Bohn, *Principles of Heat Transfer*, Brooks/Cole, CA, 2000.
9. G. R. Johnson and W. H. Cook, *Proc. 7th Int. Symp. On Ballistics*, ADPA, the Netherlands, 1983.